coatings

MDPI

Article

Investigation of Coating Performance of UV-Curable Hybrid Polymers Containing 1H,1H,2H,2H-Perfluorooctyltriethoxysilane Coated on Aluminum Substrates

Mustafa Çakır

Department of Metallurgical and Materials Engineering, Faculty of Technology, Marmara University, Goztepe 34722, Istanbul, Turkey; mcakir@marmara.edu.tr; Tel.: +90-216-336-5770 (ext. 1359)

Academic Editor: Rita B. Figueira
Received: 31 December 2016; Accepted: 22 February 2017; Published: 2 March 2017

Abstract: This study describes preparation and characterization of fluorine-containing organic-inorganic hybrid coatings. The organic part consists of bisphenol-A glycerolate (1 glycerol/phenol) diacrylate resin and 1,6-hexanediol diacrylate reactive diluent. The inorganically rich part comprises trimethoxysilane-terminated urethane, 1H,1H,2H,2H-perfluorooctyltriethoxysilane, 3-(trimethoxysilyl) propyl methacrylate and sol–gel precursors that are products of hydrolysis and condensation reactions. Bisphenol-A glycerolate (1 glycerol/phenol) diacrylate resin was added to the inorganic part in predetermined amounts. The resultant mixture was utilized in the preparation of free films as well as coatings on aluminum substrates. Thermal and mechanical tests such as DSC, thermo-gravimetric analysis (TGA), and tensile and shore D hardness tests were performed on free films. Water contact angle, gloss, Taber abrasion test, cross-cut and tubular impact tests were conducted on the coated samples. SEM examination and EDS analysis was performed on the fractured surfaces of free films. The hybrid coatings on the aluminum sheets gave rise to properties such as moderately glossed surface; low wear rate and hydrophobicity. Tensile strength of free films increased with up to 10% inorganic content in the hybrid structure and this increase was approximately three times that of the control sample. As expected; the % strain value decreased by 17.3 with the increase in inorganic content and elastic modulus values increased by a factor of approximately 6. Resistance to ketone-based solvents was proven and an increase in hardness was observed as the ratio of the inorganic part increased. Samples which contain 10% sol–gel content were observed to provide optimal properties.

Keywords: fluoropolymer coating; organic-inorganic hybrid; UV curable

1. Introduction

Aluminum and its alloys have superior properties as they are lightweight and have high thermal and electrical conductivity. Aluminum and aluminum alloys are of remarkable industrial and economic importance [1–4]. However, surfaces of unalloyed aluminum sheets have low scratch and abrasion resistance. Polymer-based coatings such as organic–inorganic hybrids are the proposed solutions for elimination of these shortcomings without losing the natural appearance. Hybrids originating from epoxy and urethane systems have been developed in recent years [5–8].

Organic–inorganic hybrid coating materials have become increasingly important materials due to their extraordinary properties such as resistance to scratching and abrasion, thermal stability, and higher chemical stability [9,10]. Hybrid materials derive these advantages from the synergy between the properties of each individual component [11]. Generally, the sol–gel route is utilized for the

preparation of organic–inorganic hybrid materials. Various organo-metal precursors based on silicone, titanium, aluminum and zirconium have been used in sol–gel processes for synthesis of the inorganic part [12,13]. Organic–inorganic hybrid materials are cured generally thermally. However, the UV curing process has been used as an alternative to thermal curing in the preparation of hybrid materials for decades [14–16].

UV-curable coatings have various advantages such as higher chemical stability, lower harm for environment, lower process costs and higher cure rates. These types of coatings have been widely used on a variety of substrates such as paper, metal, plastic and wood since the curing process is achieved using low temperatures. UV-curable coating systems can be modified by incorporating different monomeric groups. Utilization of fluorosilane structures is one of the effective methods for modification of UV-curable systems, especially for the improvement of surface characteristics [17–21].

The use of fluorinated monomers and oligomers for coatings has attracted considerable attention owing to the peculiar characteristics provided by the presence of fluorine atoms. Fluorinated coatings have hydrophobicity, chemical stability, weathering resistance, low refractive indices, good release properties, low coefficients of friction, water impermeability, low surface free energies and non-stick properties [22–24].

In this study, organic–inorganic hybrid formulations were employed, for which the inorganic part consisted of silane-terminated diethylene glycol, 1H,1H,2H,2H-perfluorooctyl triethoxysilane and 3-(trimethoxysilyl)propyl methacrylate. The organic part consisted of bisphenol-A glycerolate (1 glycerol/phenol) diacrylate and 1,6 hexanediol diacrylate. In the organic part, 3-(trimethoxysilyl) propyl methacrylate has two different roles in the hybrid formulation; on one hand, it links covalently to functional groups of silane-terminated diethylene glycol by means of Si–O–Si bonds and on the other hand it provides methylacrylate groups that allow co-polymerization with the acrylic monomer during a UV-curing process [25]. Another component present in the sol–gel precursors is 1H,1H,2H,2H-perfluorooctyltriethoxysilanes. The main role of that component in the structure is to make the organic part hydrophobic. UV-curable hybrid materials were characterized using various methods such as gloss, cross-cut, water contact angle, hardness, Taber abrasion test, tubular impact test and tensile test. Morphology and thermal properties were also investigated.

2. Experimental

2.1. Materials

Bisphenol-A glycerolate (1 glycerol/phenol) diacrylate (Bis-GA), 1.6 hexanediol diacrylate (HDDA), 3-isocyanatopropyl trimethoxysilane 95% (ICPTMS), diethylene glycol $\geq$ 99.5% (DEG), dibutyltin dilaurate, 3-(trimethoxysilyl) propyl methacrylate 98% (MEMO), 1-hydroxy-cyclohexyl-phenyl-ketone and p-toluenesulfonic acid (PTSA) were all obtained from Sigma-Aldrich. In addition, 1H,1H,2H,2H-perfluorooctyltriethoxysilane 97% (PTES) was purchased from ABCR. Anode-oxidized aluminum sheets (100 mm $\times$ 50 mm $\times$ 1 mm) were used as substrates in all coating applications.

2.2. Synthesis of Silane-Terminated Diethylene Glycol

Firstly, 5 g of diethylene glycol was charged to a 100-mL three-necked round bottom flask which was fitted with a thermometer pocket, water condenser and a magnetic stirrer. Then, 23.3094 g of 3-isocyanatopropyl trimethoxysilane was slowly added to the reaction flask. Dibutyltin dilaurate was added to the reaction flask as a catalyst at a concentration of 0.5%. The temperature was then raised to 60 °C and the mixture was stirred for 8 h. Completion of the urethane reaction was confirmed by the disappearance of the characteristic isocyanate (NCO) peak at 2275 cm^{-1} in the FT-IR spectrum.

2.3. Modification of Silane-Terminated Diethylene Glycol

A 250-mL three necked round bottom flask, equipped with a magnetic stirrer, a dropping funnel and a nitrogen inlet, was filled with 24.0461 g of 1H,1H,2H,2H-perfluorooctyl triethoxysilane (PTES),

35.0918 g of 3-(trimethoxysilyl)propyl methacrylate (MEMO) and 28.3094 g of silane-terminated diethylene glycol (STDEG). Ethanol was added to the reaction mixture. The mixture was then homogenized by mixing with a magnetic stirrer. The water/silicone ratio was calculated as $r = 3$ and the calculated amount of water was added to the mixture. Paratoluenesulfonic acid corresponding to 0.1 wt % of the above mixture was added as catalyst. The mixture was stirred for 4 h at room temperature with a magnetic stirrer. A schematic representation of the modification of STDEG is given in Figure 1. In this formulation, 3-(trimethoxysilyl) propyl methacrylate in the inorganic part has two different roles. In one of the roles, it links covalently to hydroxyl groups of STDEG by means of Si–O–Si bonds, the other role; it provides methylacrylate groups that allows co-polymerization with the acrylic monomer during a UV-curing process. Another component contained in the sol–gel precursors is 1H,1H,2H,2H-perfluorooctyltriethoxysilane. The main role of that component in the structure is to make the organic part hydrophobic.

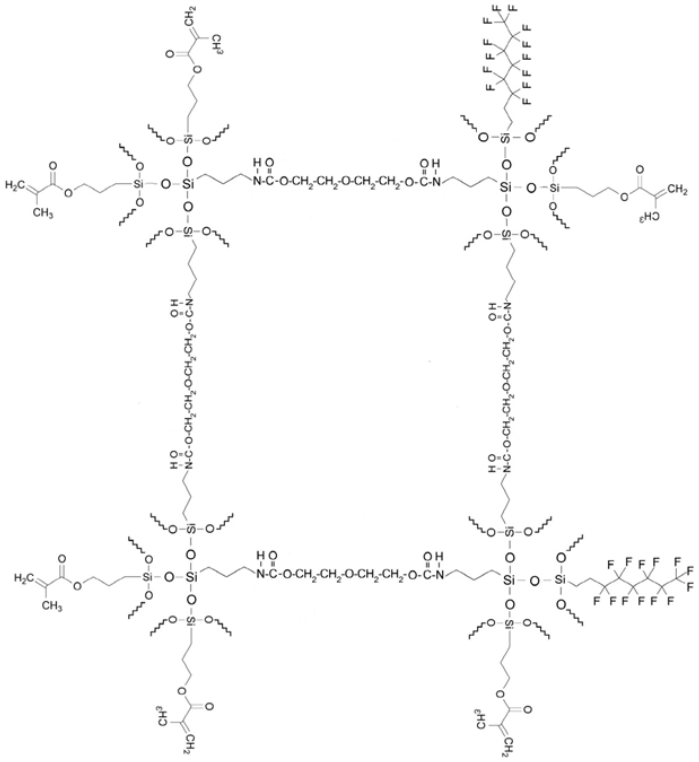

Figure 1. Schematic representation of silane-terminated diethylene glycol (STDEG) modified by both 1H,1H,2H,2H-perfluorooctyl triethoxysilane (PTES) and 3-(trimethoxysilyl)propyl methacrylate (MEMO).

2.4. Preparation of Hybrid Coatings

Hybrid coating mixtures were prepared by adding pre-hydrolyzed PTES, MEMO and STDEG to the organic part in predetermined (2.5 wt %, 5 wt %, 7.5 wt %, 10 wt %, 15 wt % and 20 wt %) ratios. The organic part of formulation comprised a UV-curable resin (Bis-GA) and a reactive diluent (HDDA). Compositions of hybrid coatings are presented in Table 1. A 3 wt % this photoinitiator was added to each of the hybrid compositions. Each composition was stirred until all the components were miscibilised completely. The efficiency of mixing was assessed by the amount of cloudiness visible during the mixing. Hybrid compositions were heated at 35 °C in a vacuum oven for about 10 min to remove the trapped air formed during the mixing process. These solutions were applied onto aluminum sheets by using a wire wound bar applicator to obtain a layer thickness of 30 μm. The obtained coatings were cured by a Raycon UV drying system with a medium pressure mercury

lamp (150 W/cm, λ_{max}: 320–390 nm), whereas the speed of conveyor belt was 5 m/min. Free films were prepared by pouring the UV curable hybrid formulations into a mold made out of Teflon® (supplied by DuPont, İstanbul, Turkey) with dimensions 10 mm × 100 mm × 1 mm. The free films were cured by passing the Teflon mold through the UV drying system under similar curing conditions applied to that of coatings.

Table 1. Composition of hybrid coatings. Bis-GA: bisphenol-A glycerolate (1 glycerol/phenol) diacrylate; HDDA: 1.6 hexanediol diacrylate.

Notation	Organic Part		Sol–Gel Precursors			Photoinitiator
	Bis-GA (wt %)	HDDA (wt %)	PTES (wt %)	MEMO (wt %)	STDEG (wt %)	Irgacure 184 Total (wt %)
S-0	80	20	–	–	–	3
S-2.5	78	19.5	0.6874	1.0032	0.8093	3
S-5	76	19	1.3748	2.0064	1.6186	3
S-7.5	74	18.5	2.0623	3.0096	2.4279	3
S-10	72	18	2.7497	4.0129	3.2373	3
S-15	68	17	4.1246	6.0193	4.8559	3
S-20	64	16	5.4995	8.0258	6.4746	3

2.5. Characterization

The FT-IR spectrum of the silane-terminated diethylene glycol was recorded on a Shimadzu 8300 FT-IR spectrophotometer (Shimadzu, Kyoto, Japan). The soluble gel content of the UV-cured free films was determined by soxhlet extraction method for 8 h using pure acetone. Insoluble gel fraction was dried in vacuum oven at 80 °C to constant weight and the soluble gel content was calculated. Thermo-gravimetric analysis (TGA) of the UV-cured free films was performed by using a Perkin Elmer thermo-gravimetric analyzer (Perkin Elmer, Waltham, MA, USA). The tests were run from 30 to 800 °C with a heating rate of 20 °C/min under an air atmosphere. DSC analysis of the hybrid films was performed by using Perkin Elmer DSC equipment (Perkin Elmer, Waltham, MA, USA). The tests were run from 20 to 220 °C with a heating rate of 10 °C/min under a N_2 atmosphere. The fracture surface of the free films was examined on JOEL JSM-5910 LV SEM equipment (Joel, Tokyo, Japan). Elemental concentrations of silicon, fluorine, carbon and oxygen atoms were determined by means of an Oxford Instruments-INCA energy dispersive spectrum (EDS) system (Oxford Instruments, Oxfordshire, UK). Water contact angles were measured by using a Krüss DSA-2 goniometer (Krüss, Hamburg, Germany). The volume of droplets was controlled to be about 3 μL. Gloss property of the coated surfaces was measured by using a BYK-Gardner Glossmeter (BYK-Gardner, Geretsried, Germany) at an angle of 60°. Mechanical properties of the specimens were determined by standard tensile test to measure the modulus (E), tensile strength (σ) and elongation at break (ε). Tensile experiments were performed at room temperature on a materials testing system Zwick Z010, using a crosshead speed of 5 mm/min. The impact resistance was assessed by falling weight method in a tubular impact tester (Sheen Instruments, Surrey, UK) (ISO 6272), 908 g weight, 25" Tube BS 6496-84. The solvent resistance of coatings was examined by performing the methyl ethyl ketone (MEK) rubbing test, according to ASTM D-5402. Adhesion properties of the coated aluminum sheets were determined by cross-cut test. For this purpose, two sets of 6 cuts with a spacing of 1 mm were made perpendicular to each other, thus making a lattice of 25 small blocks. Adhesion of coatings was determined through a tape adhesion test according to ASTM D-3359 standard by using a TESA™ 4124 tape. Then, a standardized tape was stuck on the lattice and pulled off with a constant force. The number of blocks removed was an indication of the adhesion. Hardness of free films was measured using a Zwick hardness tester (Zwick, Ulm, Germany). This test was performed according to ASTM D-2240 using Shore-D scale. The abrasion resistance of the coatings was determined by using a standardized Taber

abrasion tester (Taber Industries, New York, NY, USA) ASTM D4060. CS-10 wheels were used with a 500-g load on each wheel, and the substrates were abraded at 100, 200 and 300 cycles.

3. Results and Discussion

Completion of the urethane reaction was confirmed by the disappearance of the characteristic NCO peak at 2275 cm^{-1}, 3339 cm^{-1} stretching N–H, 1692 cm^{-1}, C=O associated urethane and isocyanurate ring stretch in the FT-IR spectrum, as shown in Figure 2.

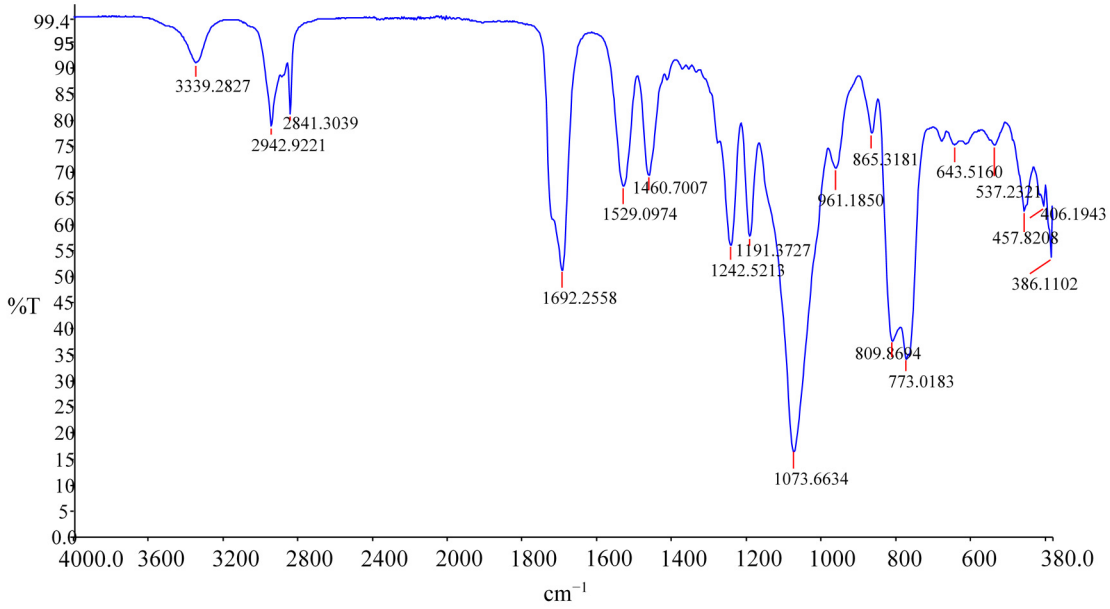

Figure 2. FT-IR spectrum of silane terminated diethylene glycol.

Figure 3 shows the contact angles of UV-cured coatings as a function of sol–gel content in the coating formulation. The contact angles of the hybrid coatings increased with the increase in sol–gel content, because the sol–gel formulation contained a high proportion of fluorine which was added to increase the hydrophobicity of the coating. The water contact angle of the control sample was 56.86°. With the incorporation of only 2.5 wt % sol–gel content, the contact angle increased to 85.97°. Only a very small amount of fluorine content significantly affected the contact angle. The water contact angle reached 98.71° at 15% sol–gel content. These results suggested that the CF_3 groups in hybrid coating increased the contact angle values. When the contact angle value of the surface is greater than 90°, the surface can be called hydrophobic [26,27]. Therefore coatings having sol–gel content greater than 5% can be considered within the class of hydrophobic coatings.

Gloss measures the amount of light reflected from a surface at a given angle and it is a significant coating property when the primary concern is aesthetics or decorative appearance. Surface roughness in clear coating influences gloss to a significant extent [28]. Besides surface roughness, gloss is also affected by the topographical orientation of the microfacets and refractive index of the coatings. The higher refractive index is, the higher surface gloss generally becomes [29]. The gloss values of the coatings were measured at 60° according to ASTM D523. The gloss values of control samples (S-0) were measured as 98.8. Increases in gloss were observed with increasing sol–gel content in the coating formulation. Among the previous studies, Tang et al [30] stated that increasing fluorine rate led to a rise in the value of gloss. Gloss value reached up to 109 in the sample with 20% sol–gel content. All gloss values can be seen in Table 2. Mulazim et al. [20] used PTES in their formulation. While they found the highest value at 107 for gloss 60°, the highest value for gloss 20° was found to be 86.

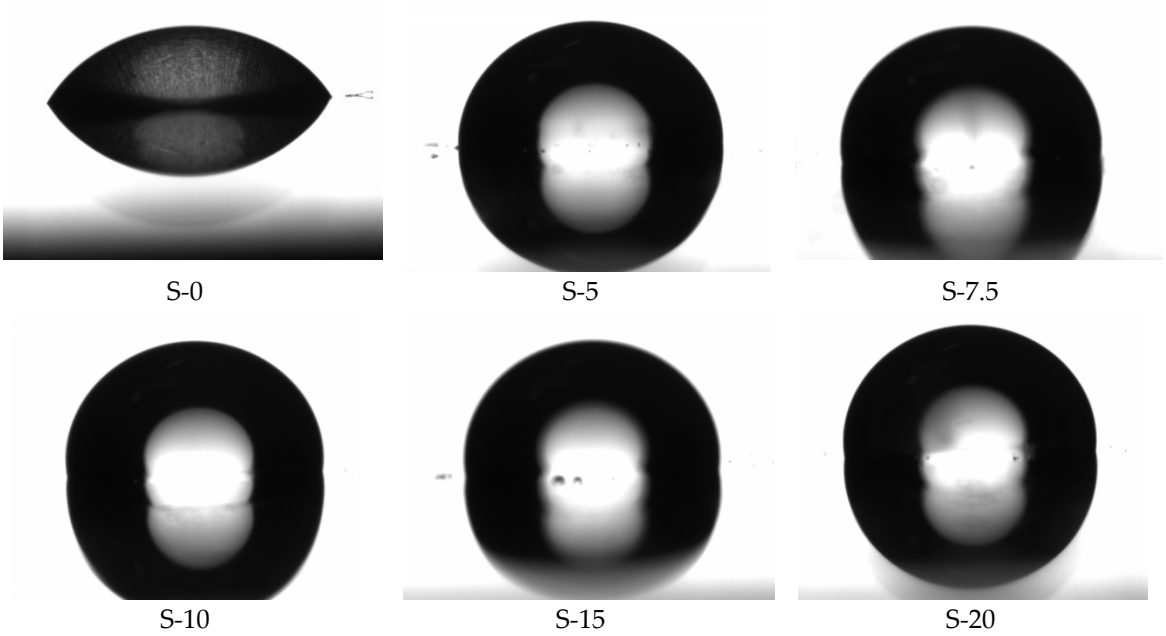

Figure 3. Contact angles of the UV-cured coatings depending on sol–gel content.

Table 2. Some of the physical properties of coatings.

Notation	Water Contact Angle	Gloss 60°	Cross-Cut ASTM D-3002	Impact Test (inch)	Hardness Shore-D	Soxhlet Extraction (% solid)	MEK Double Rub Test
S-0	56.86	98.2	5B	2	68	99.7	200
S-2.5	85.97	102.6	5B	2	71	99.8	200
S-5	95.22	103.5	5B	3	73	99.8	250
S-7.5	97.72	104.8	5B	3	73	99.6	300
S-10	98.65	107.5	4B	2	73	99.5	300
S-15	98.71	108.9	4B	1	73	99.8	300
S-20	98.10	109	3B	1	74	99.8	300

Cross-cut adhesion test was performed on the coatings according to ASTM D-3002 to determine adhesion properties of the coatings. Decreases in adhesion properties were observed with increasing ratios of sol–gel (Table 2). The reason for these decreases was the increased fluorine content. At first glance, it may be considered that adhesion properties can be improved by increasing the ratios of fluorosilane reacting with Al_2O_3 on aluminum sheets [31]. However wettability of hybrid coating formulation is decreased by increased fluorosilane content.

The ability of the coating to resist cracking led by rapid deformation was predicted by tubular impact resistance test. An indenter of fixed weight was dropped on the test surface through a graduated guided tube in this test, and a magnification lens was used to visually examine the cracks caused by rapid impact. An indenter with a hemispherical head and a diameter of 15.9 mm and 908-g load was used to conduct the tubular impact resistance test. Figure 4 shows the images of this test. At a height of one inch, only S-15 and S-20 coatings experienced cracks. Cracks formed at S-0, S-2.5 and S-10 coatings at the two-inch height impact test. S-5 and S-7.5 coating had cracks at the impact test with a height of three inches. Coatings cracked at different heights because increasing inorganic part content caused a decrease in the toughness of coatings, leading to easily-occurring cracks. Increase of sol–gel content in S-5 and S-7.5 coatings may explain the increased adhesion strength without causing decrease in toughness.

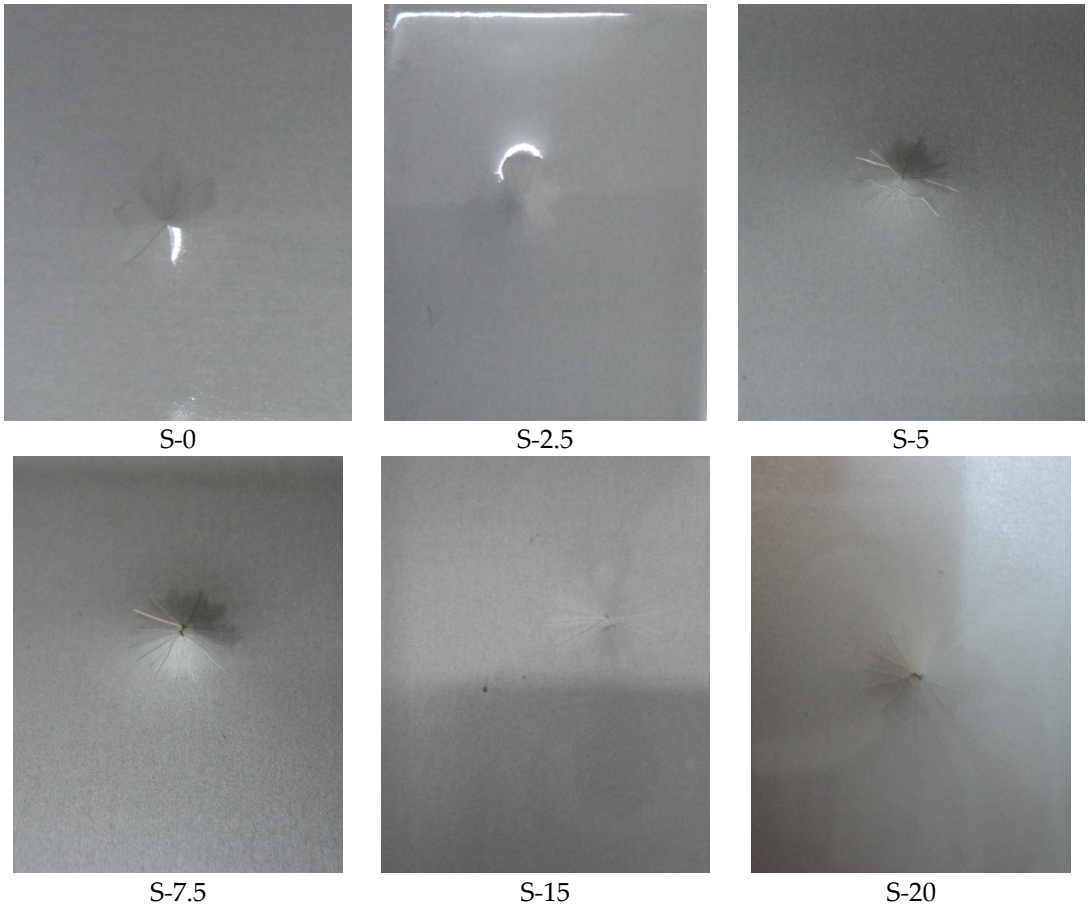

Figure 4. Picture of cracks that occurred on coatings after tubular impact test.

According to shore-D hardness test performed on free film, free film hardness values did not show significant increases by increasing sol–gel content (Table 2). The Shore-D hardness value of the S-0 sample was 68, whereas the Shore-D hardness value of the S-20 sample was 74.

UV-cured hybrid films were extracted with acetone in order to remove soluble ingredients. The weight loss of hybrid films was measured after 24 h in 80 °C in a drying process under vacuum. The solid content of the films was found to be between 99.6% and 99.8%. The solvent resistance of coatings was examined by performing MEK rubbing test, according to ASTM D-5402. MEK rubbing test values ranged from 200 to 300 cycles. Rub test values were observed to increase with increasing sol–gel content.

The sample films were prepared by free film manufacturing process in Teflon® mold. Their mechanical properties were evaluated and tabulated in Table 3. According to tensile test results, maximum tensile strength was increased with increasing sol–gel content. Tensile strength value of control sample (S-0) was 12.14 MPa. In contrast, the tensile strength value of the sample S-10 reached 31.21 MPa. An approximately threefold increase was observed in tensile strength. It was expected that elongation of coatings would decrease depending on sol–gel content.

As the fluorine-containing sol–gel content increased, % strain of the material decreased as expected. This is because inorganic materials have a lower % strain in comparison to organic materials. As the inorganic part in the hybrid structure increased, there was a decrease in % strain and it became rigid. When we examine the elastic modulus values of the samples, it is possible to see that the elasticity modulus increases with the increase of the sol–gel content. This increase in the elastic modulus provides more evidence of the hardening of the material due to the increases in sol–gel content.

Table 3. Mechanical properties of free films.

Notation	Maximum Tensile Strength (σ_M, MPa)	Strain at F_{max} (ε_M, %)	E-Modulus (E_t, MPa)
S-0	12.14	3.05	316.49
S-2.5	16.69	2.38	651.71
S-5	21.73	2.73	881.19
S-7.5	29.51	2.89	1127.96
S-10	31.21	2.85	1278.76
S-15	26.81	2.79	1427.67
S-20	19.34	2.52	1821.05

Figure 5 shows the results of the Taber abrasion test carried out using CS-10 wheels. A significant decrease was observed in weight loss due to the increases in the proportion of the fluorine-containing inorganic component. This decrease might be explained by the reduction of friction resistance due to the increase in the amount of fluorine. Previous studies have reported high abrasion resistance for coatings that have low friction resistance. The studies by McGrath et al. [32] also show decreases in friction resistance with the increasing fluorine content in the polymeric coatings.

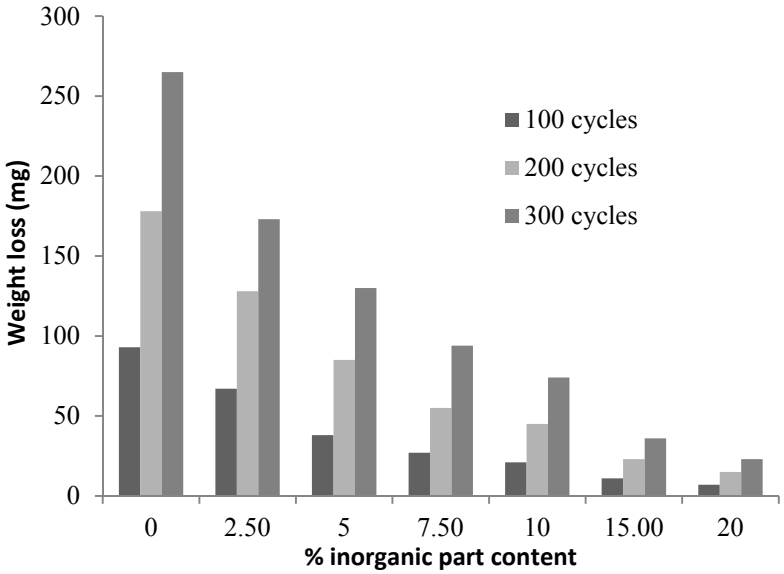

Figure 5. Abrasion resistance of coatings as a function of % inorganic part content.

Thermal properties of the hybrid films were evaluated by TGA and DSC analyses. When we examine the TGA thermograms of the hybrid films given in Figure 6, it can be seen that 10% weight loss occurs in the range of 358.5–393 °C (Table 4). 50% weight loss was at about 430 °C. Char yield increased with increasing sol–gel content as expected. However, char yield did not increase linearly with increasing inorganic part that was observed.

DSC thermograms of the samples of free films are given in Figure 7. It may be observed in Table 4 that the S-0 sample had a higher glass transition temperature (T_g = 69.27 °C) than the S-20 sample (T_g = 68.63 °C). The values of glass transition temperature (T_g) of the S-0 sample decreased with the increasing fluorine content in the inorganic part. Increases in fluorine content caused a decrease in T_g values [17,29].

SEM images of fracture surfaces of free films of the S-0, S-7.5 and S-20 samples are presented in Figure 8a–c. It is possible to see from the S-0 sample images that the unstable crack propagation took place. However, unstable crack lines were not observed on surface fracture of the S-7.5 and S-20 samples. The fracture of these samples showed a brittle tendency due to the inorganic part. It is

also possible to see that phase separation does not occur when the fractured surfaces in Figure 8b,c are examined. The inorganic phase does not precipitate as a separate region in the organic phase.

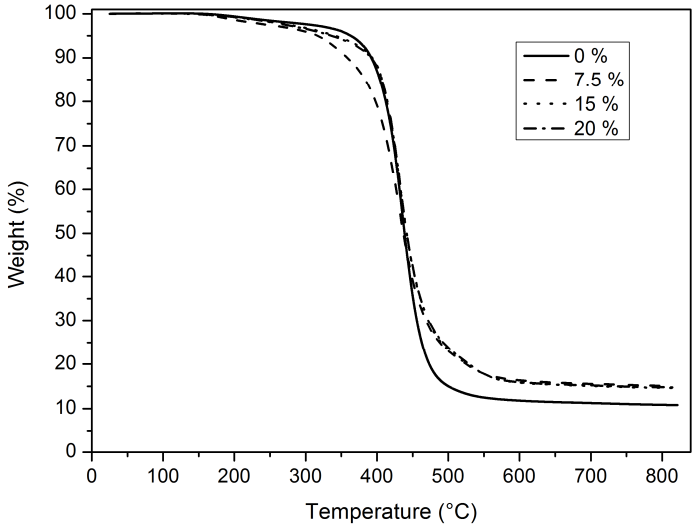

Figure 6. Thermo-gravimetric analysis (TGA) thermograms of the hybrid films.

Table 4. Thermal analysis results of UV curable hybrid films.

Notation	10% Weight Loss Temperature (°C)	50% Weight Loss Temperature (°C)	Final Weight Loss Temperature (°C)	Char Yield (%)	Glass Transition Temperature (T_g, °C)
S-0	391	438	680	10.8	69.27
S-7.5	358.5	429	685	14.66	66.49
S-15	393	434	685	14.80	68.82
S-20	391.3	427	705	15.13	68.63

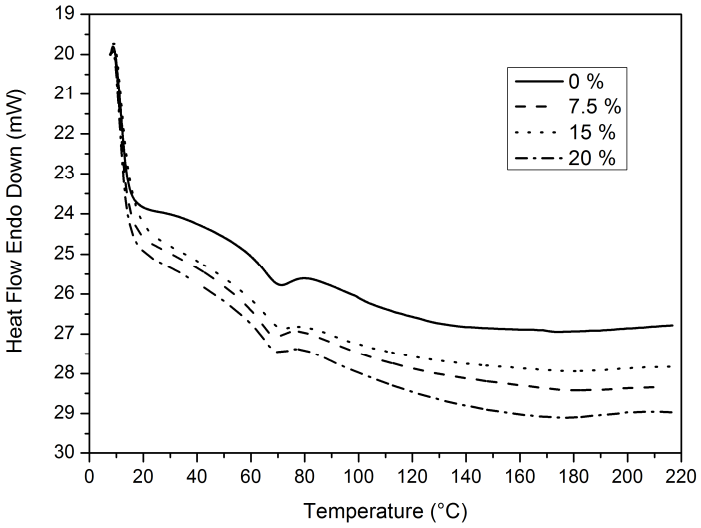

Figure 7. DSC curves of UV-curable hybrid films.

Elemental analysis of the S-20 sample was carried out by SEM-EDS analysis. SEM-EDS spectrum taken from fractured surface of the S-20 sample revealed the presence of 2.56 wt % silicon. This result confirms the effective incorporation of the inorganic precursor to the system.

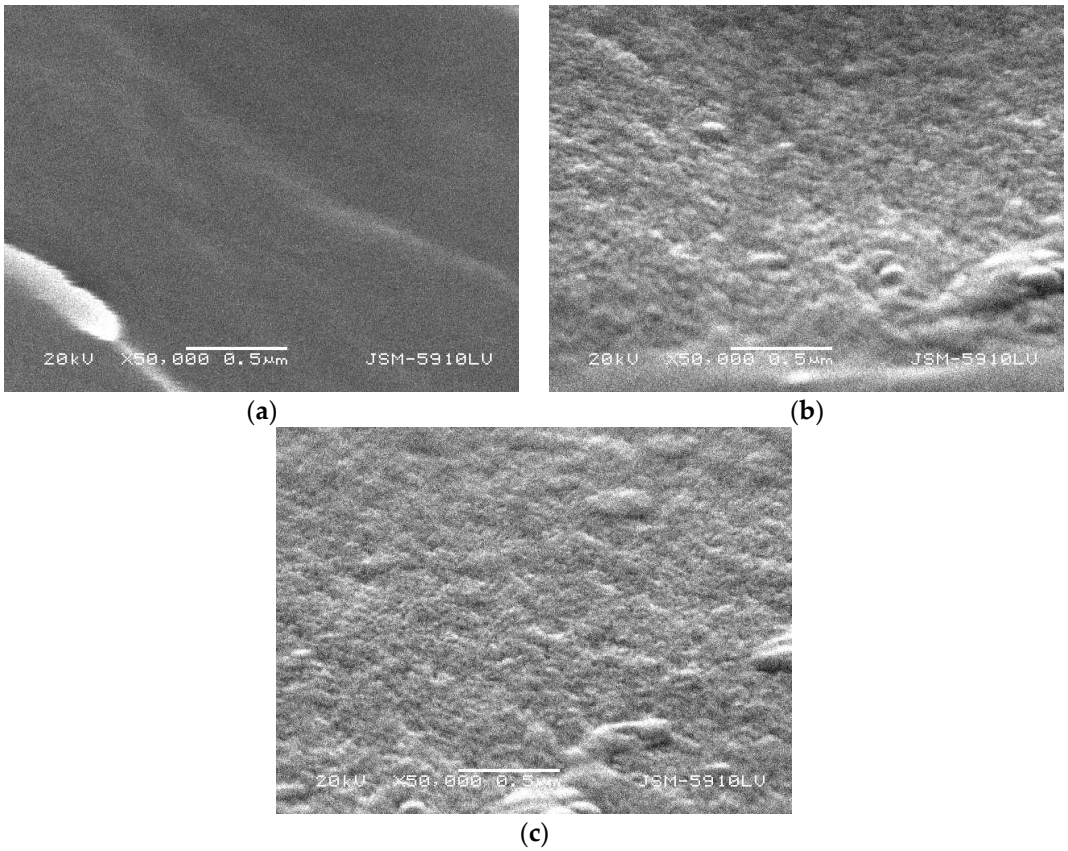

Figure 8. SEM images of the fracture surface of (**a**) S-0, (**b**) S-7.5, and (**c**) S-20 samples.

4. Conclusions

This study aimed to improve surface properties of aluminum sheets using fluorine-containing UV-curable hybrid coating formulations. Thus, hybrid coating mixtures were prepared by adding pre-hydrolyzed PTES, MEMO and STDEG to the organic part in predetermined ratios. The organic part of formulation comprised a UV-curable resin (Bis-GA), a reactive diluent (HDDA) and a photo-initiator. This prepared solution was applied onto the surface of aluminum sheets using a wire wound applicator. The coatings were then cured by passing through a UV dryer.

A significant increase was observed in the contact angles. The surfaces gained hydrophobic characteristics due to the increases in contact angles. Gloss 60° measurement values increased in parallel to the increases in the fluorine-containing inorganic part. Wear resistance of aluminum was improved without losing its natural appearance and gloss. Its resistance to ketone-based solvents was proven and an increase in hardness was observed as the ratio of the inorganic component increased. As expected, the tubular impact test values decreased with the increase in inorganic content. The adhesion of the coating to the aluminum surface was observed to be good up to an inorganic ratio of 10%, but it decreased after this ratio was exceeded. Tensile strength of free films increased with up to 10% inorganic content, and this increase reached approximately three times that of the pure sample at 31.21 MPa. As expected, the % strain value decreased by 17.3 with the increase in inorganic content and elastic modulus values increased by a factor of approximately 6. An approximately 1 °C decrease was observed in the T_g value by the increase in fluorine-containing sol–gel mixtures. Likewise, char efficiency in TGA analysis values rose from 10.8 to the value of 15.13. Considering all values mentioned above, the S-10 sample containing 10% sol–gel content was observed to provide optimal properties. It may be suggested that the formulation of the S-10 sample is suitable for coatings used for protecting the original appearance of aluminum sheets.

Conflicts of Interest: The author declares no conflict of interest.

References

1. Despic, A.; Parkhutik, V.P. Electrochemistry of Aluminum in Aqueous Solutions and Physics of Its Anodic Oxide. In *Modern Aspects of Electrochemistry*; Bockris, J.O.M., Conway, B.E., White, R.E., Eds.; Plenum Publishing: New York, NY, USA, 1989; No. 20; pp. 401–503.
2. Sheffer, M.; Groysman, A.; Mandler, D. Electrodeposition of sol–gel films on Al for corrosion protection. *Corros. Sci.* **2003**, *45*, 2893–2904. [CrossRef]
3. Ashassi-Sorkhabi, H.; Ghasemi, Z.; Seifzadeh, D. The inhibition effect of some amino acids towards the corrosion of aluminum in 1 M HCl + 1 M H_2SO_4 solution. *Appl. Surf. Sci.* **2005**, *249*, 408–418. [CrossRef]
4. Wernick, S.; Pinner, R.; Sheasby, P.G. The surface treatment of aluminum and its alloys. *ASM Int.* **1987**, *1987*, 1264.
5. Du, Y.J.; Damron, M.; Tang, G.; Zheng, H.; Chu, C.-J.; Osborne, J.H. Inorganic/organic hybrid coatings for aircraft aluminum alloy substrates. *Prog. Org. Coat.* **2001**, *41*, 226–232.
6. Liu, H.; Zheng, S.; Nie, K. Morphology and thermomechanical properties of organic–inorganic hybrid composites involving epoxy resin and an incompletely condensed polyhedral oligomeric silsesquioxane. *Macromolecules* **2005**, *38*, 5088–5097. [CrossRef]
7. Xu, J.; Pang, W.; Shi, W. Synthesis of UV-curable organic–inorganic hybrid urethane acrylates and properties of cured films. *Thin Solid Films* **2006**, *514*, 69–75. [CrossRef]
8. Pathak, S.S.; Sharma, A.; Khanna, A.S. Value addition to waterborne polyurethane resin by silicone modification for developing high performance coating on aluminum alloy. *Prog. Org. Coat.* **2009**, *65*, 206–216. [CrossRef]
9. Wen, J.; Wilkes, G.L. Organic/inorganic hybrid network materials by the sol-gel approach. *Chem. Mater.* **1996**, *8*, 1667–1681. [CrossRef]
10. Zandi-zand, R.; Ershad-langroudi, A.; Rahimi, A. Silica based organic–inorganic hybrid nanocomposite coatings for corrosion protection. *Prog. Org. Coat.* **2005**, *53*, 286–291. [CrossRef]
11. Sanchez, C.; Soler-Illia, A.; Ribot, F.; Lalot, T.; Mayer, C.R.; Cabuil, V. Designed hybrid organic-inorganic nanocomposites from functional nanobuilding blocks. *Chem. Mater.* **2001**, *13*, 3061–3083. [CrossRef]
12. Karatas, S.; Kayaman-Apohan, N.; Turunc, O.; Gungor, A. Synthesis and characterization of UV-curable phosphorus containing hybrid materials prepared by sol–gel technique. *Polym. Adv. Technol.* **2011**, *22*, 567–576. [CrossRef]
13. Tshabalala, M.A.; Sung, L.-P. Wood surface modification by in-situ sol-gel deposition of hybrid inorganic–organic thin film. *J. Coat. Technol. Res.* **2007**, *4*, 483–490. [CrossRef]
14. Zhang, L.; Zeng, Z.; Yang, J.; Chen, Y. Structure–property behavior of UV-curable polyepoxy-acrylate hybrid materials prepared via sol–gel process. *J. Appl. Polym. Sci.* **2003**, *87*, 1654–1659. [CrossRef]
15. Soppera, O.; Croutxe, C. Real-time fourier transform infrared study of free-radical UV-induced polymerization of hybrid sol–gel. I. Effect of silicate backbone on photopolymerization kinetics. *J. Polym. Sci. Part A Polym. Chem.* **2003**, *41*, 716–724. [CrossRef]
16. Kahraman, M.V.; Kugu, M.; Menceloglu, Y.; Kayaman-Apohan, N.; Gungor, A. The novel use of organo alkoxy silane for the synthesis of organic–inorganic hybrid coatings. *J. Non-Cryst. Solids* **2006**, *352*, 2143–2151. [CrossRef]
17. Beytut, H.; Cakir, M.; Kartal, I.; Sengul, M.; Tutak, D. Investigation of properties of fluorine containing hybrid coatings intended for use in printing. *Asian J. Chem.* **2015**, *27*, 3854–3860. [CrossRef]
18. Wang, T.; Isimjan, T.T.; Chen, J.; Rohani, S. Transparent nanostructured coatings with UV-shielding and superhydrophobicity properties. *Nanotechnology* **2011**, *22*, 265708. [CrossRef] [PubMed]
19. Yavas, H.; Öztürk, S.C.D.; Özhan, A.E.S.; Durucan, C. A parametric study on processing of scratch resistant hybrid sol–gel silica coatings on polycarbonate. *Thin Solid Films* **2014**, *556*, 112–119. [CrossRef]
20. Mulazim, Y.; Cakmakcı, E.; Kahraman, M.V. Photo-curable highly water-repellent nanocomposite coatings. *J. Vinyl Addit. Technol.* **2013**, *10*, 31–38. [CrossRef]
21. Park, S.; Nam, S.; Kim, L.; Park, M.; Kim, J.; An, T.K.; Yun, W.M.; Jang, J.; Hwang, J.; Park, C.E. Synthesis and characterization of a fluorinated oligosiloxane-containing encapsulation material for organic field-effect transistors, prepared via a non-hydrolytic sol–gel process. *Org. Electron.* **2012**, *13*, 2786–2792. [CrossRef]

22. Sangermano, M.; Bongiovanni, R.; Malucelli, G.; Priola, A.; Pollicino, A.; Recca, A. Fluorinated epoxides as surface modifying agents of UV-curable systems. *J. Appl. Polym. Sci.* **2003**, *89*, 1524–1529. [CrossRef]
23. Bongiovanni, R.; Malucelli, G.; Sangermano, M.; Priola, A. Properties of UV-curable coatings containing fuorinated acrylic structure. *Prog. Org. Coat.* **1999**, *36*, 70–78. [CrossRef]
24. Lin, Y.-H.; Liao, K.-H.; Huang, C.-K.; Chou, N.-K.; Wang, S.-S.; Chu, S.-H.; Hsieh, K.-H. Superhydrophobic films of UV-curable fluorinated epoxy acrylate resins. *Polym. Int.* **2010**, *59*, 1205–1211. [CrossRef]
25. Chang, C.-C.; Lin, Z.-M.; Huang, S.-H.; Cheng, L.-P. Preparation of highly transparent 13F-modified nano-silica/polymer hydrophobic hard coatings on plastic substrates. *J. Appl. Sci. Eng.* **2015**, *18*, 387–394.
26. Lau, K.K.S.; Bico, J.; Teo, K.B.K.; Chhowalla, M.; Amaratunga, G.A.J.; Milne, W.I.; McKinley, G.H.; Gleason, K.K. Superhydrophobic carbon nanotube forests. *Nano Lett.* **2003**, *3*, 1701–1705. [CrossRef]
27. Bhushan, B.; Jung, Y.C. Wetting study of patterned surfaces for superhydrophobicity. *Ultramicroscopy* **2007**, *107*, 1033–1041. [CrossRef] [PubMed]
28. Decker, C.; Keller, L.; Zahouily, K.; Benfarhi, S. Synthesis of nanocomposite polymers by UV-radiation curing. *Polymer* **2005**, *46*, 6640–6648. [CrossRef]
29. Kahraman, M.V.; Bayramoğlu, G.; Boztoprak, Y.; Güngör, A. Synthesis of fluorinated/methacrylated epoxy based oligomers and investigation of its performance in the UV curable hybrid coatings. *Prog. Org. Coat.* **2009**, *66*, 52–58. [CrossRef]
30. Tang, C.; Liu, W.; Ma, S.; Wang, Z.; Hu, C. Synthesis of UV-curable polysiloxanes containing methacryloxy/fluorinated side groups and the performances of their cured composite coatings. *Prog. Org. Coat.* **2010**, *69*, 359–365. [CrossRef]
31. Saleema, N.; Sarkar, D.K.; Gallant, D.; Paynter, R.W.; Chen, X.-G. Chemical nature of superhydrophobic aluminum alloy surfaces produced via a one-step process using fluoroalkyl-silane in a base medium. *ACS Appl. Mater. Interfaces* **2011**, *3*, 4775–4781. [CrossRef] [PubMed]
32. Kim, Y.-S.; Lee, J.-S.; Ji, Q.; McGrath, J.E. Surface properties of fluorinated oxetane polyol modified polyurethane block copolymers. *Polymer* **2002**, *43*, 7161–7170. [CrossRef]